LONG-TERM MONITORING OF THE DISTRIBUTION OF A BUILDING'S SETTLEMENTS: SECTORIZATION AND STUDY OF THE UNDERLYING FACTORS

Jesús González-Arteaga[a], Juan Alonso[a]; Marina Moya[a], Oscar Merlo[a]; Vicente Navarro[a], Ángel Yustres* [a]

Institute of Technology, University of Castilla - La Mancha, 16071 Cuenca, Campus Universitario s/n, Spain

*** Corresponding author:** angel.yustres@uclm.es , Civil Engineering School, Institute of Technology, University of Castilla - La Mancha, 16071 Campus Universitario s/n, Cuenca, Spain

González-Arteaga, J., Alonso, J., Moya, M., Merlo, O., Navarro, V., Yustres, Á., Long-term monitoring of the distribution of a building's settlements: Sectorization and study of the underlying factors (2020) Engineering Structures, 205, art. no. 110111,

DOI: https://doi.org/10.1016/j.engstruct.2019.110111

ABSTRACT

The monitoring of the structural behaviour of singular buildings and the environmental variables that affect them is an upward trend on a global scale. This paper presents a monitoring project of the building of the Institute of Technology (IT) of the University of Castilla-La Mancha in Cuenca, Spain. Different monitoring actions were carried out, specifically there were installed 27 measuring points of the soil water content (both outside and under the building), 4 clinometers with thermometers, a weather station, and 22 points for topographical levelling, thirteen of which are located on the footings of the building. Although 3 of the clinometers recorded data marked almost entirely by the evolution of the interior temperature, the one located in Module 4 showed a more complex behaviour. In order to determine the possible underlying causes of this behaviour, the footings were grouped according to the evolution of the settlements obtained by differential levelling. For this purpose, a novel clustering technique based on the calculation of the Jeffreys distance has been used instead of other more common dissimilarity measures. The analysis revealed a potential cause of the anomalous behaviour of a group of footings and permitted the study of the influence of temperature and other environmental and operative variables on this behaviour, allowing the detection of anomalies in the future.

KEYWORDS: buildings; monitoring; structural health; settlements; environmental variables; Jeffreys distance;

1. INTRODUCTION

The monitoring of critical infrastructures and singular buildings is a necessity and a growing trend [1-4]. As the conservation requirements of this type of construction progress, new monitoring systems are developed and implemented, many of them from the opportunities offered by the deployment of the Internet of Things (IoT) [5-8]. Public agencies, as managers of buildings of great social importance (hospitals, educational and administrative facilities) are in many cases the drivers of this development. However, the private sector is also very interested in monitoring as a means of knowing the value of its assets and avoiding their devaluation [9-11].

Structural health monitoring, including all its phases [12-15], has been developed in a sustained manner, with multiple case studies and applications [16-19]. However, the exclusively geotechnical aspects have been less studied [20, 21] due to their inherent difficulty of access. In the case of existing buildings, a drilling effort is required, especially in buildings with slab foundations [22], and in the case of new constructions it requires additional planning than usual during the project phase [23].

In this context the present paper shows the monitoring system implemented in the building of the Institute of Technology (IT) of the University of Castilla-La Mancha in the city of Cuenca, Spain. The heterogeneity of the soil (consistent on limestone cobbles, highly plastic soils and a granular fill) [24], the presence of different structural systems, the foundation of the building (mainly through single footings) and the existing problems in foundations of nearby buildings recommended the monitoring of several variables such as the water content of the soil [24], outdoor and indoor temperatures, other climatic variables, vertical movements of the footings and tilts in different points of four frames of the building.

The monitoring of soil moisture under buildings, although novel, is essential to understand their behaviour and know their structural health, especially if they are located on expansive soils [25-27]. In order to understand the evolution of this variable, a complete environmental monitoring (precipitation, temperature, wind speed, solar radiation) is necessary so that a reliable estimation of the value of evapotranspiration can be made [28, 29]. Likewise, the values of the vertical displacements of the footings of the building are also important as they are the elements of the structural group that collect the movements due to the expansive nature of the soil. In addition, the differential levelling [23] allows a precise evaluation of the evolution of the state of the foundation that can be corroborated by the installation of clinometers in key positions [23, 30, 31].

For the analysis of the data collected, an initial processing of the data series has been carried out for their temporal homogenisation. After that, the similarity between the series has been studied using Jeffreys distance, rather than other more commonly used metrics such as euclidean or the correlation distances [32]. From these distances, the series that potentially presented a greater similarity have been detected and clustering was carried out according to the results obtained.

Clustering techniques have been used in geotechnical problems; they have mainly been used to differentiate groups of samples of different materials [33, 34]. However, they have also been used to transfer these groupings to the spatial dimension, with the delimitation of geotechnical units in a map [35, 36] or for the delineation of horizons in sedimentary materials [37] from in situ tests with vertical distributions of measurements. They have also been used to obtain homogeneous groups of variables that allow the use of artificial intelligence techniques (artificial neural networks) for the prediction of the settlement of shallow foundations on granular soils [38]. In the present work this technique however has been used for the clustering of structural behaviours (settlement of the footings) of the studied building. From the obtained results, a zoning was made and with it the detection of a potential pathology related to the construction phase.

The proposed methodology can be used in the future, once new data are obtained, to detect changes in behaviour and to establish alert or corrective action thresholds [14].

2. MONITORING ACTIONS

For the study of the behaviour of the IT building several magnitudes have been measured, using materials and methods both conventional and innovative. For the case of the distribution of soil moisture under the building and its surroundings has been developed a methodology [24] based on the use of the Frequency Domain Reflectometry (FDR) with measurement ports drilled in hard soils [39]. A total of 26 measurement points were available (Figure 1) with data up to 120 cm deep spaced every 10 cm vertically. Measurements were made by an operator on irregularly distributed days, but with an average cadence of 15 days (Figure 2).

The official records of AEMET (Spanish State Agency of Meteorology) in the city of Cuenca and the SIAR (regional service of advice to irrigators) in the nearby town of Mariana have been used for the environmental and climate monitoring. Both official meteorological stations are located 1.97 and 9.85 kilometres respectively from the studied building. However to complement these records an own weather station (Decagon Weather Station, DWS, [40]) was set up. The own environmental data were taken with a frequency of 15 minutes, as compared to the daily frequency of the official climate data of AEMET and the service of the SIAR. However, the own data did not cover the whole study period (Figure 2). Since the IT building is composed of four modules (Figure 1), it was considered necessary to record the evolution of the indoor temperature of each of them. The temperature sensors were built-in to the clinometers, so their spatial location is coincident.

A differential levelling was performed using a Topcon AT-B2 automatic level equipped with an optical micrometer and a 2 m invar levelling staff, to measure the relative elevation of a total of 22 points, of which 14 are located on the building's footings (Figure 1 for L_i points). The misclosure error was always below the permissible error (0.296 mm), calculated by the expression [41]

$$\sigma = \sigma_{ran}\sqrt{L} \quad (1)$$

where σ is the allowable misclosure, σ_{ran} (mm) is the random error accumulated over one kilometre of levelling and L (km) is the total distance of the levelling loop. For this case the values of σ_{ran} = 0.5 mm and L = 0.34941 km were taken.

Finally, four clinometers of type EL-SC (Durham Geo Slope Indicator [42]) named C_1 to C_4 were installed in four beams of their respective roof frames in each of the modules of the building. Their precise location can be seen in Figure 1. For the installation of the clinometers, the location of the anchors was marked. The holes were drilled in the structure (Figure 3a), and once cleaned the holes were filled with epoxy grout and the anchors (Figure 3b) were inserted. In the meantime, the omni bracket was screwed to a 2m rigid metal beam (Figure 3c). Then the tilt sensor was attached to the omni bracket (Figure 3d). After that the beam was mounted on the anchor bolts (Figure 3e) using a bubble level to check horizontality (Figure 3f). Finally the sensor was connected and calibrated, registering the values with a datalogger (Figure 3g). For clinometer C_1 the omni bracket was attached to a steel beam directly (Figure 3h). The structural typology in which these devices are located is different: clinometer C_1 is in a metallic structure, C_2 and C_3 are located in a frame of reinforced concrete with a one-way hollow block slab and C_4 was located in a reinforced concrete waffle slab. A differentiated response is therefore expected, especially with the variation of the indoor temperature. The tilt angles were recorded every 15 minutes, with the same time frequency of measurement as the temperature.

As it was advanced for the case of outdoor climate monitoring, all the series of measurements do not have the same time extension, since the systems were implemented throughout 27 months. Figure 2 shows the time coverage of each of the records, as well as the irregular spacing of the differential levelling and soil moisture data. From this temporal distribution, the series corresponding to the external environmental variables of AEMET, the internal temperatures, the water contents in the soil, the results of the differential levelling and the tilt angles measured by the clinometers were selected for their study. The study period runs from 18 October 2016 to 27 June 2018, for which all series have data, except for the own weather station. However, it was found that the values of this station corresponded very satisfactorily with the official daily values recorded by AEMET, so it was decided to use this station for the entire period of study. All records for which the measuring interval is less than the daily interval (e.g. monitoring instruments with automatic data acquisition) have been passed to a daily frequency by calculating the average daily value of the monitored variable. On the contrary, those with a measurement interval higher than daily (variables that require one or several human operators for their measurement) have been completed by means of a linear interpolation between the available data. Thus, all series have a total of 618 readings, one per day.

3. METHODS FOR DATA ANALYSIS.

The evolution of the vertical position of the differential levelling points shows several different trends, but due to the existing dispersion and the amount of data available, a clustering algorithm was used to obtain a more objective grouping. Initially, the distance between data sets was calculated using linear correlation [43] although unsatisfactory results were obtained due to the presence of spurious data introduced by the linear interpolation performed to fill the gaps in the series. Therefore, a quantitative way of measuring the differences in the shape of the time series of settlements was investigated and the Jeffreys distance was chosen. Initially the Jeffreys distance was designed to compare the differences in the amount of information contained in any two probability density functions (pdfs). It evaluates, the difference in the shape of the time series and not so much their correspondence point to point that pursues the correlation, thus having a better performance for interpolated series. The Jeffreys distance is defined as [44]

$$J\left(P,Q\right)=KL\left(P,Q\right)+KL\left(Q,P\right) \tag{2}$$

where *KL(P,Q)* is the Kullback-Leibler (KL) divergence measure between discrete functions *P(j)* and *Q(j)* and *KL(Q,P)* is the one between *Q(j)* and *P(j)*. Jeffreys distance is a way of symmetrizing the non-symmetrical divergence measure of Kullback-Leibler by the sum of their values in both directions (distance from P to Q and distance from Q to P). The KL divergence, as mentioned above, was designed to evaluate differences in information content between two pdfs, so its expression (for discrete functions) is given by

$$KL\left(P,Q\right)=\sum_{i}\hat{P}\left(j\right)\log\left(\frac{\hat{P}\left(j\right)}{\hat{Q}\left(j\right)}\right) \tag{3}$$

where $\hat{P}\left(j\right)$ and $\hat{Q}\left(j\right)$ are normalized and positive discrete functions. As a result, these two functions, like any other pdf-type function, have to fulfil that the sum of the probabilities is equal to the unit

$$\sum_{j}\hat{P}(j)=\sum_{j}\hat{Q}(j)=1 \tag{4}$$

and that all probability values must be positive, so that

$$\hat{P}(j)>0 \tag{5}$$

$$\hat{Q}(j)>0 \tag{6}$$

In the present case for obtaining the positive normalized functions $\hat{P}(j)$ or $\hat{Q}(j)$, the minimum value of each time series was subtracted from all data. The resulting series was divided by the sum of all its components and finally a sufficiently small value was added ($\varepsilon=1\times10^{-12}$) so that all values were greater than 0.

In order to organize all this information, the use of a hierarchical clustering algorithm of the series according to Jeffreys distances was proposed. The Ward variance minimization algorithm, widely used in various scientific applications [45-50], has been used as a linkage criterion by means of the Python routine scipy.cluster.hierarchy.linkage [51]. The method consists of identifying the two series with the shortest distance between them, in our case the aforementioned footings L_20 and L_22. Both series are linked in a group. The calculation of the existing distance between this group and the rest of series (or groups of series) is made using the expression

$$d\left(\hat{U},\hat{V}\right)=\sqrt{\frac{\left|\hat{V}\right|+\left|\hat{P}\right|}{T}d\left(\hat{V},\hat{P}\right)^{2}+\frac{\left|\hat{V}\right|+\left|\hat{Q}\right|}{T}d\left(\hat{V},\hat{Q}\right)^{2}+\frac{\left|\hat{V}\right|}{T}d\left(\hat{P},\hat{Q}\right)^{2}} \tag{7}$$

Where $d\left(\hat{U},\hat{V}\right)$ is the distance between $\hat{U}$, the new group formed from the linkage of the $\hat{P}$ and $\hat{Q}$ series, and the $\hat{V}$ series (or group of series) and where |•| denotes the cardinality of the cluster. In the case of an individual series the cardinality will be 1 and in the case of clusters, this value would be the number of series included. T denotes the total number of individual series contained in the elements $\hat{U}$ and $\hat{V}$. The two rows and columns of the initial matrix of corresponding to the series $\hat{P}$ and $\hat{Q}$ are replaced by one corresponding to the group $\hat{U}$ and consequently the matrix is reduced in dimensionality (one row and one column less) and the process is repeated. Sequentially, groups are linked and gradually the most similar series are grouped. If in a graph the names of the original series are placed in the x-axis and in the y-axis the existing distances between the linked groups are plotted (calculated by means of the Eq. 7) we obtain a graph called dendrogram. In the present work the Python routine scipy.cluster.hierarchy.dendrogram [52] has been used for this purpose.

4. RESULTS AND DISCUSSION

The Jeffreys distances obtained between all series are shown in Figure 4. As can be seen, there are series of settlements between which the distance is very low (e.g. L_20 and L_22 as expected due to their physical proximity, highlighted in red in Figure 4) and some others which present higher differences with the rest.

Following the hierarchical clustering algorithm presented in the previous section, three main groups were obtained after the analysis of the dendrogram (Figure 5). The first and second groups (Figure 6) correspond to the points located to the northwest and south of the building, with oscillating tendencies around the initial value. The third group shows a downward trend.

It is important to highlight the consistency of the proposed clusters with the structure of the foundation soil. Given that the grade plane elevation of the site was 947.5 meters above sea level, the area where the third group has been located (south and southeast of module 4 of IT building) had to be filled, while the rest had to be cut, as illustrated in

Figure 7. The filling was made with a coarse granular material with short consolidation times. For this reason, the final trend of this process has been captured by the differential levelling (Figure 6c). The Group 1 points are located in the excavated zone, therefore on the natural soil which is a clayey material with a liquid limit ranging between 42% and 62%, with a swelling index of 0.02 and a compression index of 0.08 [24]. These values indicate that it cannot be considered as a very deformable soil. These values indicate that it cannot be considered as a very deformable soil. This means that, although it experiences volume changes caused by variations in the water content (Figure 8a), by changes in the position of the water table (Figure 8b) and by interactions with the atmosphere (Figure 8c) the total settlement is small (Figure 6a). Group 2 defines the transition between the two groups defined above, between the area where it was not filled (Group 1) and the area where up to 7 meters of granular material was placed (Group 3). Since in this material the measured water content changes were negligible [24], they resulted in minor vertical movements in Group 2. Similarly, the consolidation movements associated with the construction were also lower, as the filling depth was considerably lower than in Group 1.

On the other hand, if one evaluates the distance of Jeffreys between the settlements and other such as indoor temperature (Figure 9) settlements of footings and tilt, an important phenomenon can be observed. The clinometers C_1, C_2 and C_3 present very low distances with respect to the temperature series (cells highlighted in red in Figure 10a), which indicates that the movements in the structure are mainly of thermal origin. However, in the case of the C_4 clinometer, the lowest distances (cells highlighted in red in Figure 10b) are found with the settlement records of L_13 and L_14 footings (located southeast of the building, in the southern part of Module 4). Also, consequently with the clustering performed, it presents low distances with the rest of the levelling points within

Group 4. Therefore, much of the behaviour registered by the C_4 clinometer is explained by the settlement of earthfill beneath the south and southeast of Module 4 (Figure 7). However, there must also be a thermal component, similar to that of Modules 2 and 3, since all three clinometers are placed on reinforced concrete frames. Separating both components (thermal and due to foundation settlements) in the time series of data is not a simple task, due to the limitations mentioned above: different measurement frequencies between differential levelling and C_4 clinometer data and different structural typology among the modules. The following expression is proposed

$$\theta_4^s = \frac{1}{2}\left(s_{L14}^* + s_{L15}^*\right)\left(\theta_{4,\max} - \theta_{4,\min}\right) + \theta_{4,\min} \quad (8)$$

where θ_4^s is the component of the C_4 clinometer data series caused by the settlements, $\theta_{4,\max}$ and $\theta_{4,\min}$ are the maximum and minimum values of the series recorded by this clinometer and s_{L14}^* and s_{L15}^* are the dimensionless series of settlements of L_14 and L_15 footings, which are calculated by the expression

$$s_k^*\left(j\right) = \frac{s_k\left(j\right) - s_{k,\min}}{s_{k,\max} - s_{k,\min}} \quad (9)$$

where $s_k\left(j\right)$ is jth the settlement data and $s_{k,\max}$ and $s_{k,\min}$ are the maximum and minimum values of the series of settlements of the footing *k* (L_14 or L_15). All the s_k^* series therefore range between 0 and 1 and can be summed as in Eq. 8. The factor $\frac{1}{2}\left(s_{L14}^* + s_{L15}^*\right)$ of this expression returns the mean value of the two dimensionless series, or what is the same, the shape of θ_4^s function. Furthermore, the factor $\left(\theta_{4,\max} - \theta_{4,\min}\right) + \theta_{4,\min}$ gives the scale and position of the series of tilt angles measured by the clinometer C_4. θ_4^s function is shown in Figure 11a (blue line, settlement component)

The effects of the settlement of the footings are not the only ones that should be taken into account when interpreting the evolution of the tilt recorded by clinometers. Other environmental and operational variables may affect this behaviour. Several authors [53-55] have found very strong linear correlations of temperature and displacements in different singular bridges. This linear correlation with temperature has also been detected in geotechnical works (where the role of temperature is somewhat more buffered) such as in rigidly framed earth retaining structures [56] and a concrete underground car park [57]. The detection of this linear correlation has been used in some cases to differentiate between several environmental and operational variables [58], although in general the use of more advanced techniques such as those described in [59, 60] is necessary to eliminate the influence of those variables on the estimates of modal parameters of singular structures. In the present work, the component of thermal effects is obtained from the study of the correlation between temperature and tilt recorded by clinometers C_2 and C_3 (Figure 12). For both cases the slope of the regression line is almost identical, although the intercept is slightly different. However, in the case of the metal structure, the slope is very different, as expected, implying that this value is highly dependent on the material and on its thermal expansion coefficient. Although the correlation between the tilt and the temperature is extremely dependent on the structure in which it is measured, given that Module 4 is in the same building, made of the same material, has the same constructive conditions and the same HVAC system probably presents a very similar behaviour. Consequently, for the estimation of the thermal effect on the C_4 clinometer data the same slope identified for C_2 and C_3 will be used, and the intercept will be determined by minimizing the mean of the interannual movement. Thus, the following expression is obtained

$$\theta_4^T = 6.493\times10^4 \times T - 1.144\times10^2 \qquad (10)$$

where θ_4^T is the tilt angle due to the effect of temperature and T is the value of that temperature in ºC. The function is shown in Figure 11a (green line, thermal component). Together with the settlement component they constitute the explained component of the recorded tilt, obtaining the satisfactory fit between θ_4 and $\theta_4^s + \theta_4^T$ illustrated in Figure 11b.

A synthetic structural safety index could be derived from the settlement series and the maximum allowed values of angular distortion proposed in the literature [61] or in the technical codes [62]. However, the methodology proposed in this work does allow an indirect assessment of the structural safety of the building. If the clusters change significantly over time or if new clusters appear, the presence of a new pathology could be suspected. Likewise, if the clinometers clearly lose the correlations shown in Figure 12, this suspicion would be reaffirmed. Consequently, the analysis of the data provides the basis for the diagnosis of structural health over time.

5. CONCLUSIONS

In the present work, a monitoring programme has been carried out in a building of recent construction, which has allowed the characterization of the water content beneath the foundations of the building, the settlements in several footings as well as the monitoring of the interior temperatures and the tilt in different points of the structure of the building.

In order to structure and analyse the information obtained, a hierarchical clustering process has been carried out, based on the use of the Jeffreys distance. The use of this novel technique for defining the similarity measure between two series has permitted to identify settlement trends consistent with the structure of the foundation soil and with the hydrogeological and environmental conditions. In addition, the comparison metric based on the Jeffreys distance has allowed to define the general structure of the mobilization of the building. The model obtained allows the definition of the expected trend of tilt, thus allowing the early identification of anomalous behaviours potentially associated with structural problems.

Acknowledgements

The authors acknowledge funding support from Diputación de Cuenca through the research starting grant DIPUCU-2017-7 awarded to Mr. González-Arteaga.

REFERENCES

[1] la Manna M. Monitoring and control of urban critical infrastructures. In: Tremante A, Chu H-W, Sanchez B, Callaos NC, editors. 6th International Multi-Conference on Complexity, Informatics and Cybernetics, IMCIC 2015 and 6th International Conference on Society and Information Technologies, ICSIT 2015 - Proceedings. Orlando, Florida USA International Institute of Informatics and Systemics, IIIS; 2015. p. 74-5.

[2] Meyer C, Cucino P, Eccher G, Ulrich D. The Florence high-speed railway hub: 4D monitoring - Innovations in data acquisition and data management for tunnelling projects in sensitive urban areas. In: Anagnostou G, Ehrbar H, editors. World Tunnel Congress 2013. Geneva; Switzerland: CRC Press 2013. p. 1403-10.

[3] Noel AB, Abdaoui A, Elfouly T, Ahmed MH, Badawy A, Shehata MS. Structural Health Monitoring Using Wireless Sensor Networks: A Comprehensive Survey. IEEE Communications Surveys and Tutorials. 2017;19:1403-23.

[4] Wang T, Bhuiyan MZA, Wang G, Rahman MA, Wu J, Cao J. Big Data Reduction for a Smart City's Critical Infrastructural Health Monitoring. IEEE Communications Magazine. 2018;56:128-33.

[5] Babazadeh M, Kartakis S, McCann JA. Highly-distributed sensor processing using IoT for critical infrastructure monitoring. Proceedings - 9th Asia-Pacific Signal and Information Processing Association Annual Summit and Conference, APSIPA ASC 2017. Kuala Lumpur; Malaysia: Institute of Electrical and Electronics Engineers Inc.; 2018. p. 1065-74.

[6] Lu G, Yang Y. IoT and smart infrastructure. In: Geng H, editor. Internet of Things and Data Analytics Handbook: John Wiley & Sons, Inc.; 2017. p. 481-93.

[7] Minoli D, Sohraby K, Occhiogrosso B. IoT Considerations, Requirements, and Architectures for Smart Buildings-Energy Optimization and Next-Generation Building Management Systems. IEEE Internet of Things Journal. 2017;4:269-83.

[8] Vögler M, Schleicher JM, Inzinger C, Dustdar S. Ahab: A cloud-based distributed big data analytics framework for the Internet of Things. Software - Practice and Experience. 2017;47:443-54.

[9] Dubbs NC. Expanding the Case for Structural Health Monitoring: A Focus on Its Role in Maintenance and Operations and Asset Management Systems. Structures Congress 2018: Bridges, Transportation Structures, and Nonbuilding Structures. Fort Worth; United States: American Society of Civil Engineers (ASCE); 2018. p. 197-204.

[10] Winkler J, Hendy C. Improved structural health monitoring of London's Docklands Light Railway bridges using Digital image correlation. Structural Engineering International: Journal of the International Association for Bridge and Structural Engineering (IABSE). 2017;27:435-40.

[11] Wu ZY. Developing integrated methods and software tools for monitoring-based asset performance management. In: Chang F-K, Kopsaftopoulos F, editors. 11th Structural Health Monitoring 2017: Real-Time Material State Awareness and Data-Driven Safety Assurance - Proceedings of the 11th International Workshop on Structural Health Monitoring, IWSHM 2017. Stanford University Stanford; United States: DEStech Publications; 2017. p. 197-204.

[12] Cross EJ, Worden K, Farrar CR. Structural health monitoring for civil infrastructure. In: Haldar A, editor. Health Assessment of Engineered Structures: Bridges, Buildings, and Other Infrastructures. Singapore: World Scientific Publishing Co.; 2013. p. 1-32.

[13] Worden K, Farrar CR, Manson G, Park G. The fundamental axioms of structural health monitoring. Proceedings of the Royal Society A: Mathematical, Physical and Engineering Sciences. 2007;463:1639-64.

[14] Farrar CR, Worden K. An introduction to structural health monitoring. Philosophical Transactions of the Royal Society A: Mathematical, Physical and Engineering Sciences. 2007;365:303-15.

[15] Karbhari VM. Introduction: structural health monitoring – a means to optimal design in the future. In: Karbhari VM, Ansari F, editors. Structural Health Monitoring of Civil Infrastructure Systems: Woodhead Publishing; 2009. p. xv-xxiv.

[16] Datteo A, Lucà F, Busca G. Statistical pattern recognition approach for long-time monitoring of the G.Meazza stadium by means of AR models and PCA. Engineering Structures. 2017;153:317-33.

[17] Döhler M, Hille F, Mevel L, Rücker W. Structural health monitoring with statistical methods during progressive damage test of S101 Bridge. Engineering Structures. 2014;69:183-93.

[18] Hu W-H, Caetano E, Cunha Á. Structural health monitoring of a stress-ribbon footbridge. Engineering Structures. 2013;57:578-93.

[19] Yarnold MT, Moon FL. Temperature-based structural health monitoring baseline for long-span bridges. Engineering Structures. 2015;86:157-67.

[20] Rainieri C, Fabbrocino G, Santucci de Magistris F. An Integrated Seismic Monitoring System for a Full-Scale Embedded Retaining Wall. Geotechnical Testing Journal. 2013;36:40-53.

[21] Rainieri C, Dey A, Fabbrocino G, Santucci de Magistris F. Interpretation of the experimentally measured dynamic response of an embedded retaining wall by finite element models. Measurement. 2017;104:316-25.

[22] Díaz E, Robles P, Tomás R. Multitechnical approach for damage assessment and reinforcement of buildings located on subsiding areas: Study case of a 7-story RC building in Murcia (SE Spain). Engineering Structures. 2018;173:744-57.

[23] Moore JFA. Monitoring Building Structures Glasgow, UK: Blackie and Son Ltd; 1992.

[24] Gonzalez-Arteaga J, Moya M, Yustres A, Alonso J, Merlo O, Navarro V. Characterisation of the water content distribution beneath building foundations. Measurement. 2019:82-92.

[25] Yoshida RT, Fredlund DG, Hamilton JJ. The prediction of total heave of a slab-on-ground floor on Regina clay. Canadian Geotechnical Journal. 1983;20:69-81.

[26] Briaud JL, Zhang X, Moon S. Shrink test-water content method for shrink and swell predictions. Journal of Geotechnical and Geoenvironmental Engineering. 2003;129:590-600.

[27] Adem HH, Vanapalli SK. Review of methods for predicting in situ volume change movement of expansive soil over time. Journal of Rock Mechanics and Geotechnical Engineering. 2015;7:73-86.

[28] Zhang X. Consolidation theories for saturated-unsaturated soils and numerical simulations of residential buildings on expansive soils [Ph. D.]. College Station, TX: Texas A&M University; 2004.

[29] Gens A. Soil-environment interactions in geotechnical engineering. Geotechnique. 2010;60:3-74.

[30] Xia Y, Zhang P, Ni YQ, Zhu HP. Deformation monitoring of a super-tall structure using real-time strain data. Engineering Structures. 2014;67:29-38.

[31] Sung YC, Lin TK, Chiu YT, Chang KC, Chen KL, Chang CC. A bridge safety monitoring system for prestressed composite box-girder bridges with corrugated steel webs based on in-situ loading experiments and a long-term monitoring database. Engineering Structures. 2016;126:571-85.

[32] SciPy. scipy.spatial.distance.pdist, https://docs.scipy.org/doc/scipy/reference/generated/scipy.spatial.distance.pdist.html#scipy.spatial.distance.pdist. 2019.

[33] Mayer JM, Allen DM, Gibson HD, Mackie DC. Application of statistical approaches to analyze geological, geotechnical and hydrogeological data at a fractured-rock mine site in Northern Canada. Hydrogeology Journal. 2014;22:1707-23.

[34] Viviescas JC, Osorio JP, Griffiths DV. Cluster analysis for the determination of the undrained strength tendency from SPT in mudflows and residual soils. Bulletin of Engineering Geology and the Environment. 2019;78:5039-54.

[35] Masoud AA. Geotechnical evaluation of the alluvial soils for urban land management zonation in Gharbiya governorate, Egypt. Journal of African Earth Sciences. 2015;101:360-74.

[36] Sun CG, Kim HS. GIS-based regional assessment of seismic site effects considering the spatial uncertainty of site-specific geotechnical characteristics in coastal and inland urban areas. Geomatics, Natural Hazards and Risk. 2017;8:1592-621.

[37] Rogiers B, Mallants D, Batelaan O, Gedeon M, Huysmans M, Dassargues A. Model-based classification of CPT data and automated lithostratigraphic mapping for high-resolution characterization of a heterogeneous sedimentary aquifer. PLoS ONE. 2017;12.

[38] Shahin MA, Maier HR, Jaksa MB. Data division for developing neural networks applied to geotechnical engineering. Journal of Computing in Civil Engineering. 2004;18:105-14.

[39] Navarro V, Candel M, Yustres A, Merlo O, Mena M. Analysis of installation of FDR sensors in a hard soil. Geotechnical Testing Journal. 2006;29:462-6.

[40] ICT International. DWS Decagon Weather Station. Armidale, New South Wales, Australia: ICT International,; 2019.

[41] Ogundare JO. Precision Surveying : The Principles and Geomatics Practice. Hoboken, UNITED STATES: John Wiley & Sons, Incorporated; 2015.

[42] Slope Indicator Company. EL Tilt Sensor,(For Tilt and Beam Sensors), Standard & SC Versions, 56802198. Mukilteo, Washington, USA2010. p. 30.

[43] Cha S-H. Comprehensive Survey on Distance/Similarity Measures between Probability Density Functions International Journal of Mathematical Models and Methods in Applied Sciences. 2007;1:300-3007.

[44] Nielsen F. Jeffreys centroids: A closed-form expression for positive histograms and a guaranteed tight approximation for frequency histograms. IEEE Signal Processing Letters. 2013;20:657-60.

[45] Argüelles M, Benavides C, Fernández I. A new approach to the identification of regional clusters: Hierarchical clustering on principal components. Applied Economics. 2014;46:2511-9.

[46] Konopka BM, Lwow F, Owczarz M, Łaczmański Ł. Exploratory data analysis of a clinical study group: Development of a procedure for exploring multidimensional data. PLoS ONE. 2018;13.

[47] Lyra GB, Oliveira-Júnior JF, Zeri M. Cluster analysis applied to the spatial and temporal variability of monthly rainfall in Alagoas state, Northeast of Brazil. International Journal of Climatology. 2014;34:3546-58.

[48] Martin TM, Harten P, Venkatapathy R, Das S, Young DM. A hierarchical clustering methodology for the estimation of toxicity. Toxicology Mechanisms and Methods. 2008;18:251-66.

[49] Ramachandra Rao A, Srinivas VV. Regionalization of watersheds by hybrid-cluster analysis. Journal of Hydrology. 2006;318:37-56.

[50] Rebotier TP, Prather KA. Aerosol time-of-flight mass spectrometry data analysis: A benchmark of clustering algorithms. Analytica Chimica Acta. 2007;585:38-54.

[51] Scipy. scipy.cluster.hierarchy.linkage, https://docs.scipy.org/doc/scipy/reference/generated/scipy.cluster.hierarchy.linkage.html?highlight=linkage#scipy.cluster.hierarchy.linkage. 2019.

[52] Scipy. scipy.cluster.hierarchy.dendrogram, https://docs.scipy.org/doc/scipy/reference/generated/scipy.cluster.hierarchy.dendrogram.html?highlight=dendrogram#scipy.cluster.hierarchy.dendrogram. 2019.

[53] de Battista N, Brownjohn JMW, Tan HP, Koo KY. Measuring and modelling the thermal performance of the Tamar Suspension Bridge using a wireless sensor network. Structure and Infrastructure Engineering. 2015;11:176-93.

[54] Roberts GW, Brown CJ, Tang X. Correlated GNSS and temperature measurements at 10-minute intervals on the Severn Suspension Bridge. Applied Geomatics. 2017;9:115-24.

[55] Yang DH, Yi TH, Li HN, Zhang YF. Correlation-Based Estimation Method for Cable-Stayed Bridge Girder Deflection Variability under Thermal Action. Journal of Performance of Constructed Facilities. 2018;32.

[56] Iskander M. Relationship Between Temperature and Earth Pressure for a Rigidly Framed Earth Retaining Structure. Geotech Geol Eng. 2013;31:519-39.

[57] Aboumoussa W, Iskander M. Thermal movements in concrete: Case study of multistory underground car park. Journal of Materials in Civil Engineering. 2003;15:545-53.

[58] Xia Q, Zhou L, Zhang J. Thermal performance analysis of a long-span suspension bridge with long-term monitoring data. Journal of Civil Structural Health Monitoring. 2018;8:543-53.

[59] Rainieri C, Magalhaes F. Challenging aspects in removing the influence of environmental factors on modal parameter estimates. Procedia Engineering2017. p. 2244-9.

[60] Rainieri C, Magalhaes F, Gargaro D, Fabbrocino G, Cunha A. Predicting the variability of natural frequencies and its causes by Second-Order Blind Identification. Structural Health Monitoring. 2019;18:486-507.

[61] Burland JB, Wroth CP. Settlement of buildings and associated damage. Proceedings, Conference on Settlement of Structures. 1974:611-54.

[62] Committee European Committee for Standardization (CEN). Eurocode 3: Design of steel structures - Part 1-1: General rules and rules for buildings. 1995.

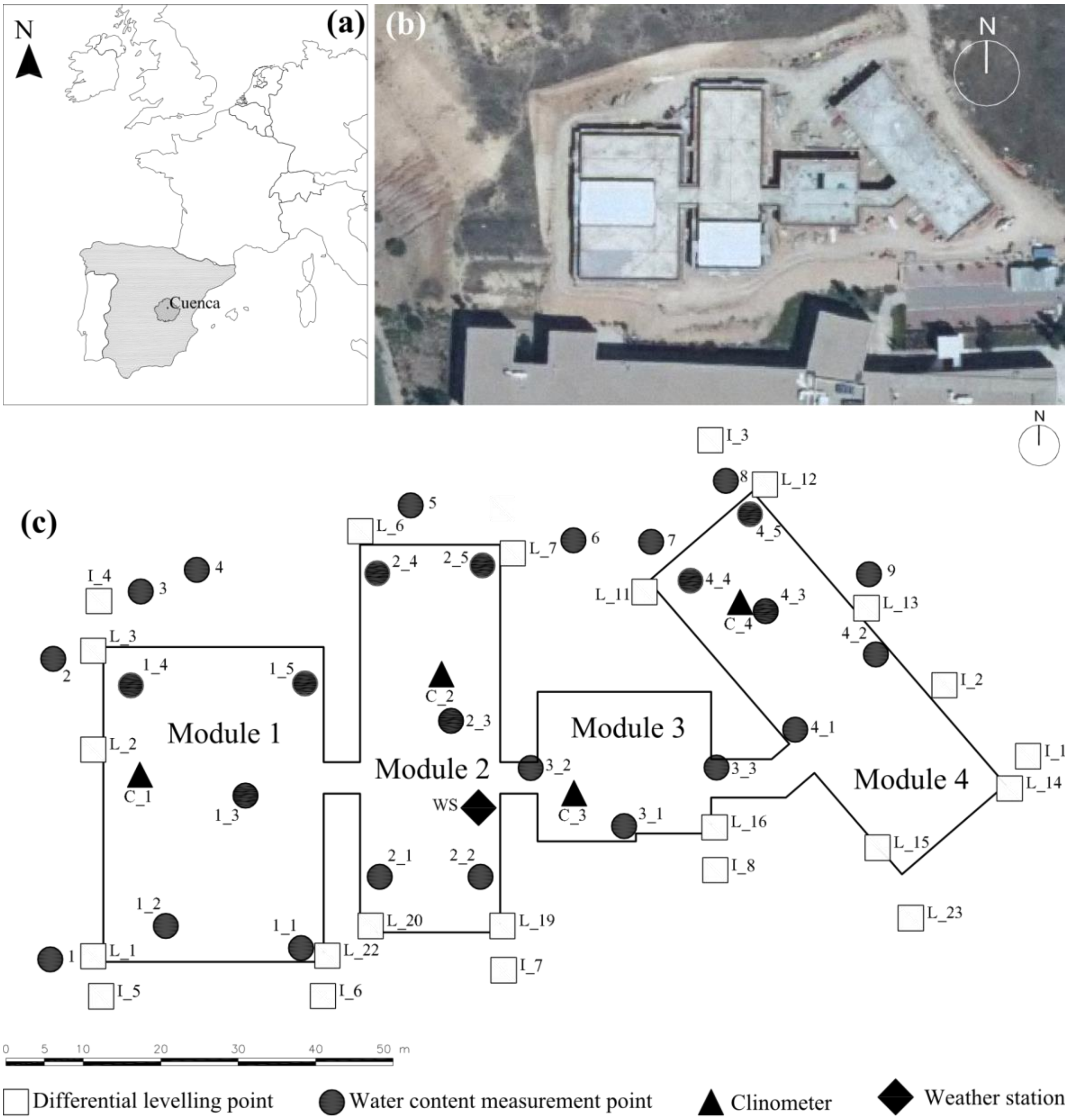

Figure 1. (a) Location, (b) Orthorectified image and (c) plan view of the position of the monitoring points.

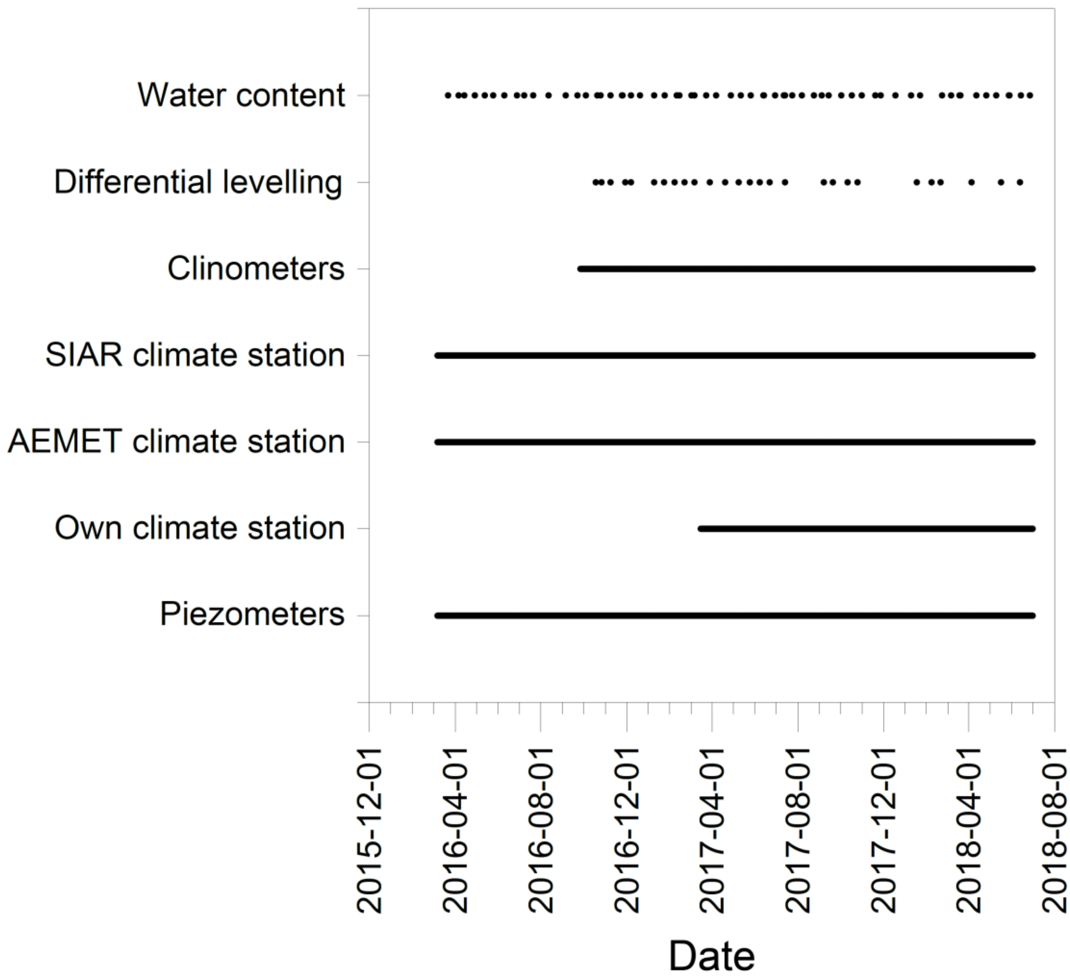

Figure 2. Time coverage of the monitoring actions.

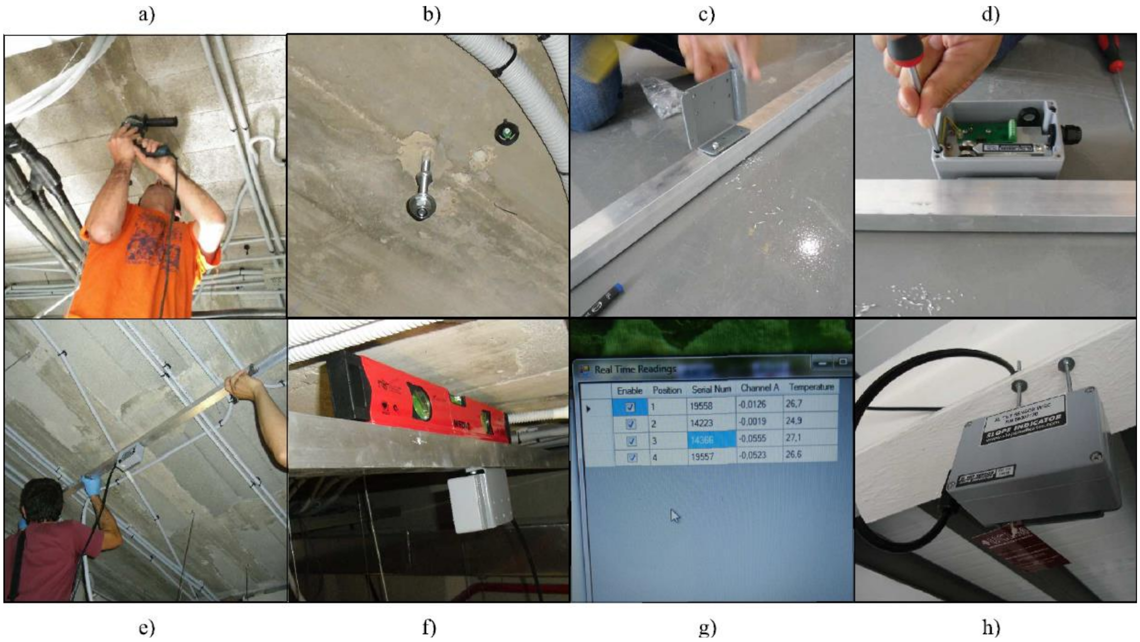

Figure 3. Installation process of clinometers. (a) Drilling of the holes in which the anchors are placed. (b) Epoxy resin filling and installation of anchors. (c) Installation of omni brackets (d) attachment of the tilt sensor to the omni bracket (e) Assembly of the 2 metre auxiliary beam in the anchors (f) Horizontality check (g) Sensor calibration (h) Direct installation (without auxiliary beam) in the metal structure of Module 1.

	L_14	I_1	I_2	L_13	L_12	I_3	L_7	L_6	I_4	L_3	L_2	L_1	I_5	I_6	L_22	L_20	I_7	L_19	I_8	L_16	L_15	L_23
L_14	0	0.062	0.030	0.072	0.378	0.555	0.495	0.514	0.483	0.494	0.557	0.347	0.215	0.554	0.457	0.488	0.661	0.371	0.118	0.435	0.106	0.329
I_1	0.062	0	0.098	0.186	0.493	0.688	0.606	0.581	0.510	0.535	0.604	0.421	0.279	0.628	0.552	0.581	0.742	0.480	0.232	0.581	0.246	0.436
I_2	0.030	0.098	0	0.116	0.507	0.695	0.650	0.658	0.584	0.641	0.733	0.469	0.296	0.707	0.608	0.649	0.805	0.487	0.211	0.575	0.184	0.396
L_13	0.072	0.186	0.116	0	0.156	0.259	0.242	0.254	0.237	0.251	0.294	0.148	0.079	0.305	0.222	0.244	0.369	0.152	0.073	0.212	0.038	0.191
L_12	0.378	0.493	0.507	0.156	0	0.026	0.012	0.019	0.077	0.042	0.053	0.029	0.077	0.072	0.034	0.031	0.092	0.012	0.202	0.046	0.145	0.173
I_3	0.555	0.688	0.695	0.259	0.026	0	0.021	0.019	0.071	0.055	0.059	0.070	0.142	0.073	0.045	0.042	0.076	0.040	0.327	0.072	0.259	0.249
L_7	0.495	0.606	0.650	0.242	0.012	0.021	0	0.011	0.089	0.047	0.056	0.053	0.120	0.053	0.029	0.024	0.058	0.023	0.283	0.042	0.212	0.203
L_6	0.514	0.581	0.658	0.254	0.019	0.019	0.011	0	0.047	0.034	0.040	0.052	0.118	0.055	0.035	0.026	0.053	0.027	0.306	0.068	0.243	0.207
I_4	0.483	0.510	0.584	0.237	0.077	0.071	0.089	0.047	0	0.071	0.085	0.083	0.098	0.086	0.066	0.066	0.085	0.067	0.301	0.134	0.255	0.204
L_3	0.494	0.535	0.641	0.251	0.042	0.055	0.047	0.034	0.071	0	0.007	0.024	0.086	0.100	0.059	0.048	0.117	0.042	0.276	0.100	0.261	0.232
L_2	0.557	0.604	0.733	0.294	0.053	0.059	0.056	0.040	0.085	0.007	0	0.037	0.124	0.110	0.066	0.047	0.128	0.056	0.298	0.118	0.298	0.290
L_1	0.347	0.421	0.469	0.148	0.029	0.070	0.053	0.052	0.083	0.024	0.037	0	0.039	0.100	0.051	0.050	0.142	0.033	0.175	0.087	0.151	0.176
I_5	0.215	0.279	0.296	0.079	0.077	0.142	0.120	0.118	0.098	0.086	0.124	0.039	0	0.124	0.082	0.097	0.177	0.056	0.132	0.109	0.090	0.108
I_6	0.554	0.628	0.707	0.305	0.072	0.073	0.053	0.055	0.086	0.100	0.110	0.100	0.124	0	0.019	0.026	0.026	0.068	0.319	0.072	0.245	0.185
L_22	0.457	0.552	0.608	0.222	0.034	0.045	0.029	0.035	0.066	0.059	0.066	0.051	0.082	0.019	0	0.005	0.044	0.032	0.235	0.041	0.174	0.162
L_20	0.488	0.581	0.649	0.244	0.031	0.042	0.024	0.026	0.066	0.048	0.047	0.050	0.097	0.026	0.005	0	0.042	0.025	0.251	0.035	0.190	0.167
I_7	0.661	0.742	0.805	0.369	0.092	0.076	0.058	0.053	0.085	0.117	0.128	0.142	0.177	0.026	0.044	0.042	0	0.078	0.431	0.082	0.314	0.196
L_19	0.371	0.480	0.487	0.152	0.012	0.040	0.023	0.027	0.067	0.042	0.056	0.033	0.056	0.068	0.032	0.025	0.078	0	0.211	0.028	0.137	0.107
I_8	0.118	0.232	0.211	0.073	0.202	0.327	0.283	0.306	0.301	0.276	0.298	0.175	0.132	0.319	0.235	0.251	0.431	0.211	0	0.256	0.045	0.280
L_16	0.435	0.581	0.575	0.212	0.046	0.072	0.042	0.068	0.134	0.100	0.118	0.087	0.109	0.072	0.041	0.035	0.082	0.028	0.256	0	0.148	0.098
L_15	0.106	0.246	0.184	0.038	0.145	0.259	0.212	0.243	0.255	0.261	0.298	0.151	0.090	0.245	0.174	0.190	0.314	0.137	0.045	0.148	0	0.140
L_23	0.329	0.436	0.396	0.191	0.173	0.249	0.203	0.207	0.204	0.232	0.290	0.176	0.108	0.185	0.162	0.167	0.196	0.107	0.280	0.098	0.140	0

Figure 4. Jeffreys distances existing between the series of settlements at the levelling points (L_i for footings and I_i for auxiliary points). Highlighted in red the minimal values found between footings L_20 and L_22.

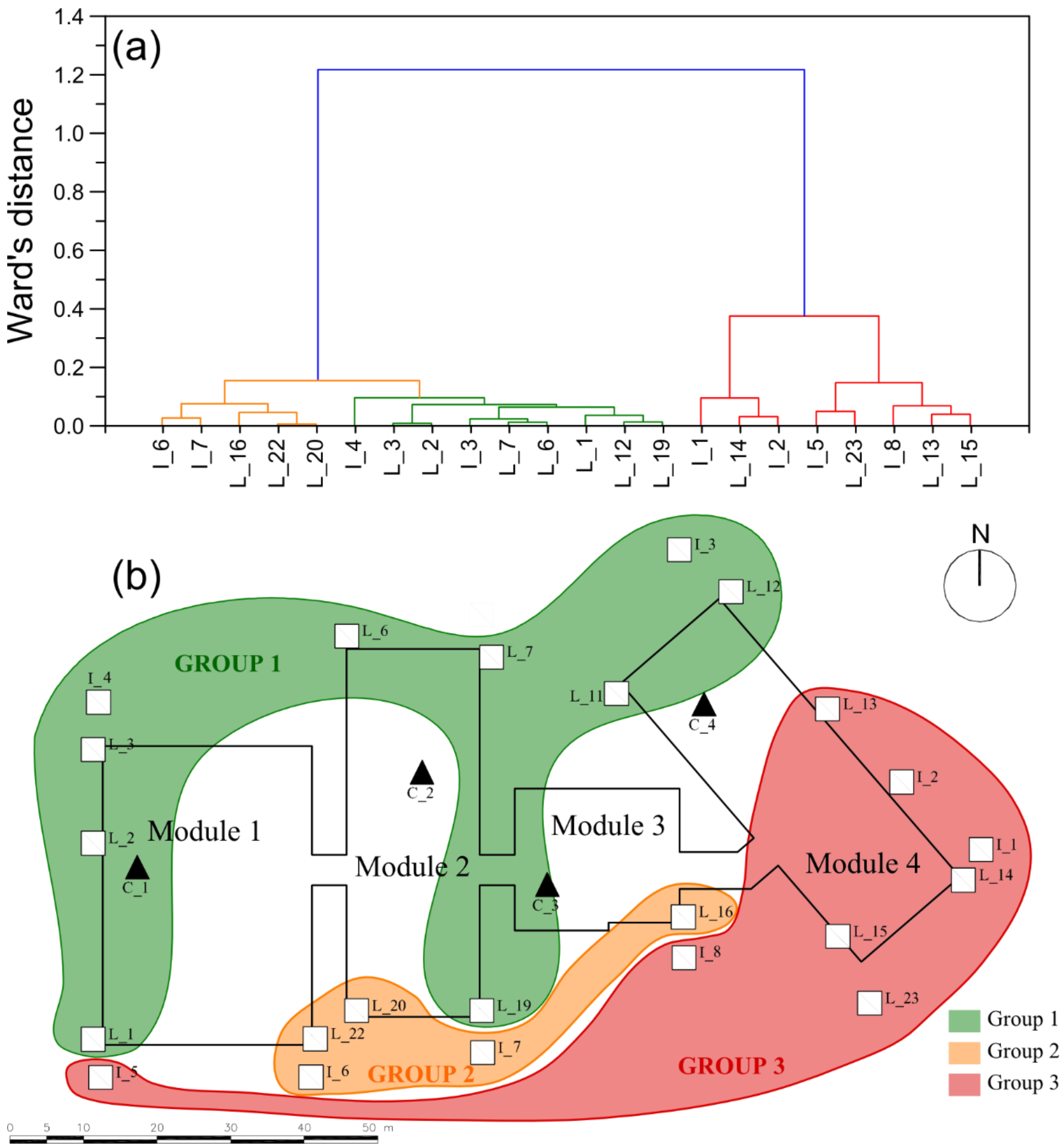

Figure 5. Grouping of levelling points. (a) Proposed dendrogram (b) Spatial distribution.

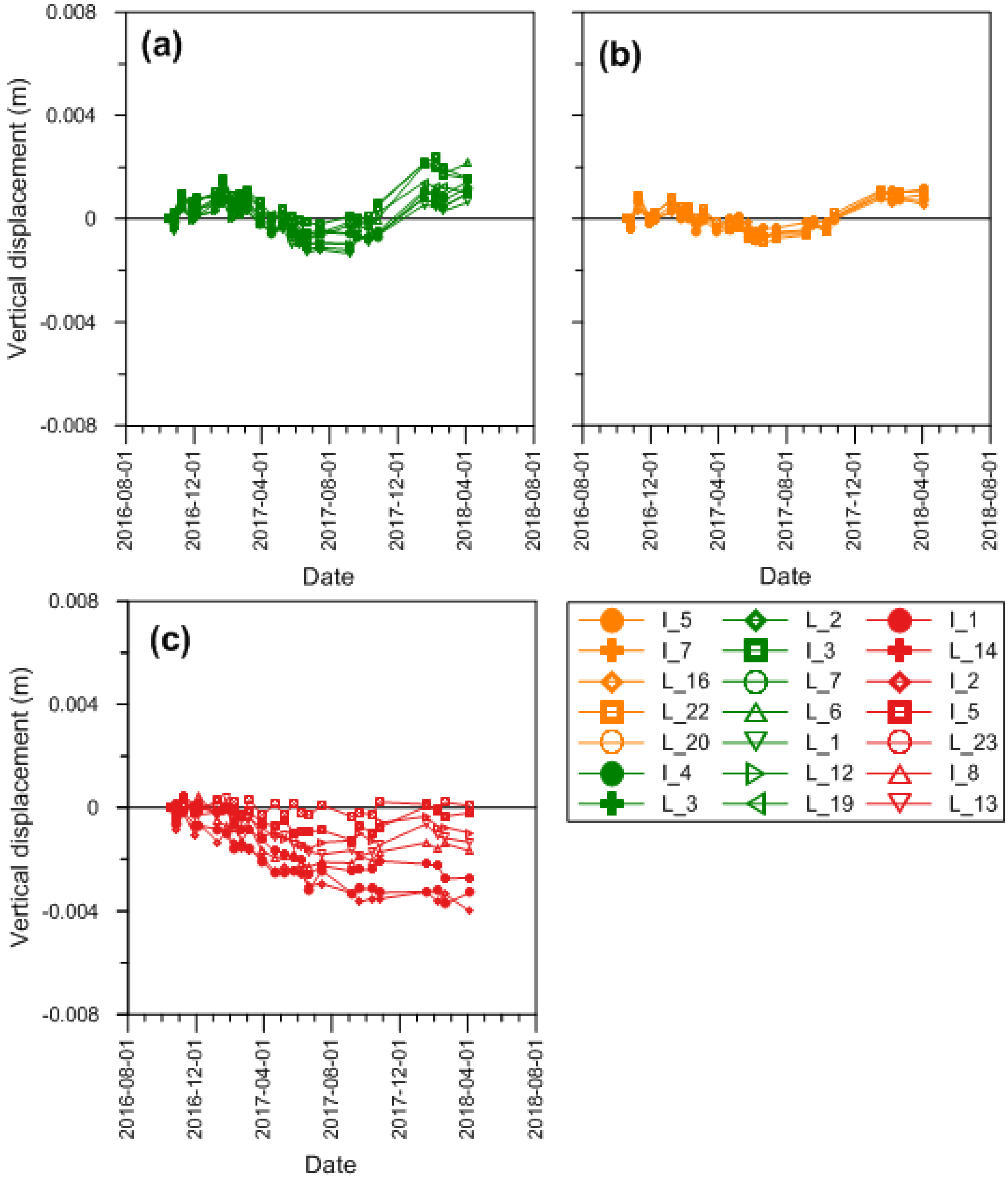

Figure 6. Evolution of the vertical displacements with respect to the initial position according to the groups identified in Figure 5. (a) Group 1 (b) Group 2 (c) Group 3

Figure 7. Distribution of the cut-off (purple) and fill (green) areas on the plot where the building is located.

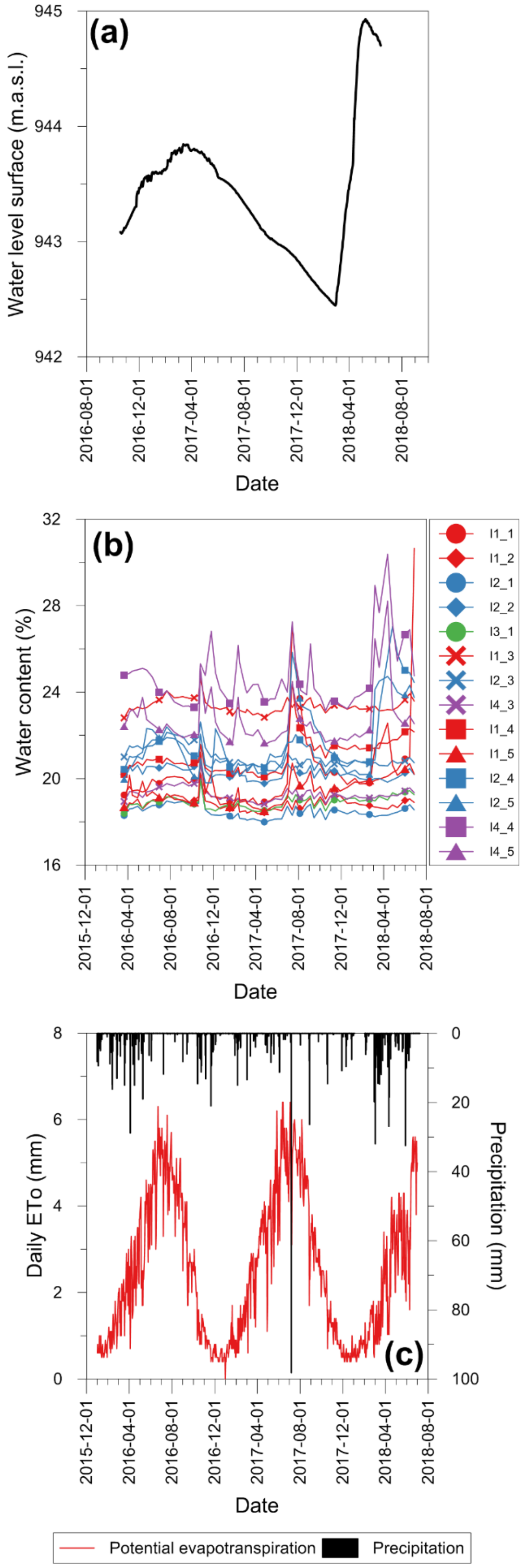

Figure 8. (a) Fluctuation of the water table below the study area (b) Evolution of the water content beneath the foundation of the building at different points (c) Evolution of potential evapotranspiration and precipitation recorded in the study period

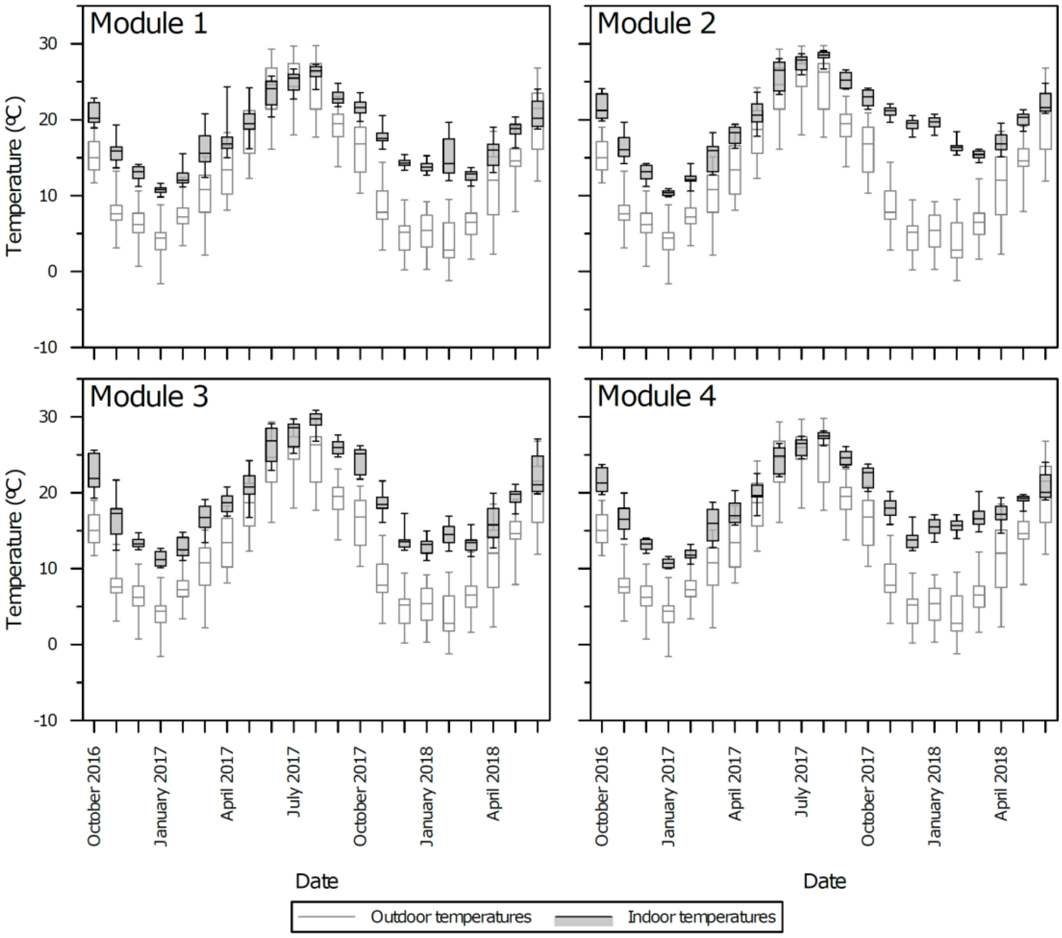

Figure 9. Outdoor and indoor temperatures of each of the four modules.

(a)

	T_1	T_2	T_3	T_4	C_1	C_2	C_3	C_4
T_1	0	0.030	0.017	0.023	0.014	0.055	0.040	0.802
T_2	0.030	0	0.051	0.023	0.062	0.014	0.050	0.862
T_3	0.017	0.051	0	0.026	0.032	0.082	0.035	0.864
T_4	0.023	0.023	0.026	0	0.050	0.042	0.043	0.851
C_1	0.014	0.062	0.032	0.050	0	0.090	0.047	0.679
C_2	0.055	0.014	0.082	0.042	0.090	0	0.069	0.952
C_3	0.040	0.050	0.035	0.043	0.047	0.069	0	0.741
C_4	0.802	0.862	0.864	0.851	0.679	0.952	0.741	0

(b)

	T_1	T_2	T_3	T_4	C_1	C_2	C_3	C_4
L_14	0.696	0.775	0.753	0.763	0.560	0.867	0.636	0.090
I_1	0.616	0.724	0.653	0.683	0.501	0.816	0.575	0.138
I_2	0.705	0.793	0.753	0.771	0.558	0.899	0.668	0.126
L_13	0.731	0.751	0.817	0.765	0.607	0.799	0.656	0.111
L_12	0.826	0.776	0.936	0.821	0.762	0.741	0.726	0.355
I_3	0.953	0.871	1.069	0.926	0.912	0.822	0.841	0.503
L_7	0.819	0.743	0.930	0.797	0.785	0.697	0.728	0.460
L_6	0.820	0.757	0.930	0.797	0.776	0.704	0.732	0.470
I_4	0.774	0.719	0.877	0.747	0.730	0.689	0.705	0.458
L_3	0.958	0.906	1.071	0.945	0.894	0.876	0.861	0.367
L_2	1.130	1.063	1.256	1.109	1.066	1.020	1.014	0.436
L_1	0.868	0.834	0.971	0.866	0.789	0.821	0.771	0.275
I_5	0.646	0.625	0.732	0.649	0.575	0.646	0.576	0.180
I_6	0.698	0.621	0.791	0.658	0.676	0.579	0.598	0.544
L_22	0.752	0.686	0.851	0.727	0.712	0.653	0.653	0.435
L_20	0.821	0.752	0.924	0.793	0.777	0.705	0.712	0.466
I_7	0.693	0.605	0.792	0.649	0.686	0.544	0.616	0.636
L_19	0.721	0.663	0.826	0.709	0.671	0.638	0.642	0.336
I_8	0.940	0.964	1.022	0.962	0.821	1.028	0.847	0.176
L_16	0.705	0.630	0.814	0.694	0.664	0.590	0.613	0.423
L_15	0.686	0.694	0.766	0.707	0.582	0.735	0.601	0.178
L_23	0.447	0.407	0.531	0.449	0.410	0.406	0.410	0.348

Figure 10. Jeffreys distances between . (a) between the time series of indoor temperature (T_i) and tilt of the clinometers (C_i). Highlighted in red the distances between indoor temperatures and the tilt registered in the corresponding clinometers. (b) the time series of settlements at the levelling points (L_i and I_i), indoor temperature (T_i) and tilt of the clinometers (C_i). Highlighted in red the small distances between settlements in footings L_13 and L_14 and the tilt registered in clinometer C4

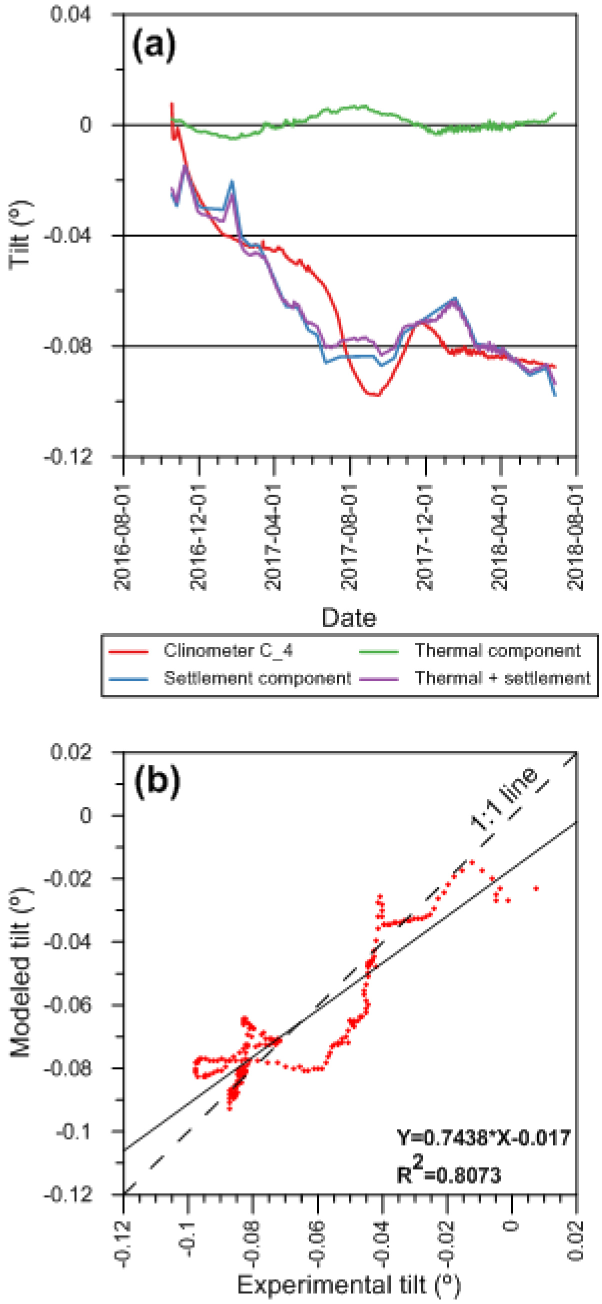

Figure 11. Proposal for the decomposition of the measured tilts.

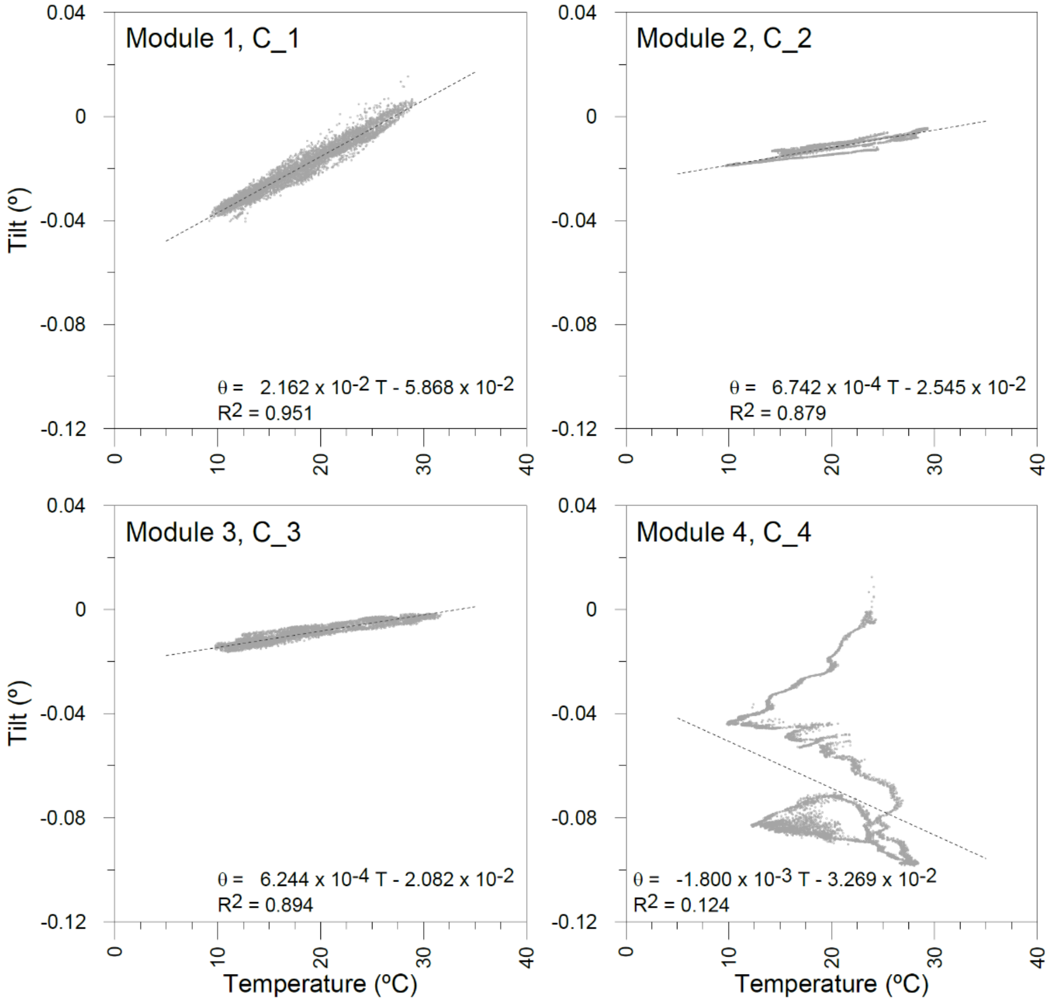

Figure 12. Correlations and regression lines identified between the tilt measured by clinometers and the temperature of each of the building's modules.